Evaporation and condensation processes of giant molecular clouds in a hot plasma

Wolfgang Vieser (`vieser@astrophysik.uni-kiel.de`) and
Gerhard Hensler (`hensler@astrophysik.uni-kiel.de`)
Institut für Theor. Physik und Astrophysik, Universität Kiel, D - 24098 Kiel, Germany

Abstract. 2D hydrodynamical simulations are performed to examine the evaporation and condensation processes of giant molecular clouds in the hot phase of the interstellar medium. The evolution of cold and dense clouds ($T = 1000$ K, $n_H = 3$ cm^{-3}, $M = 6 \cdot 10^4$ M$_\odot$) is calculated in the subsonic stream of a hot tenuous plasma ($T = 5 \cdot 10^6$ K, $n_H = 6 \cdot 10^{-4}$ cm^{-3}). Our code includes self-gravity, heating and cooling processes and heat conduction by electrons. The thermal conductivity of a fully ionized hydrogen plasma ($\kappa \propto \mathrm{T}^{5/2}$) is applied as well as a saturated heat flux in regions where the mean free path of the electrons is large compared to the temperature scaleheight.

Significant differences occur between simulations with and without heat conduction. In the simulations without heat conduction, the clouds outermost regions is stired up by Kelvin-Helmholtz (KH) instability after only a few dynamical times. This prevents an infiltration of a significant amount of hot gas into the cloud before its destruction. In contrast, models including heat conduction evolve less violently. The boundary of the cloud remains nearly unsusceptible to KH instabilities. In this scenario it is possible to mix the formerly hot streaming gas very effectively with the cloud material.

Keywords: evaporation, condensation, heat conduction, molecular clouds

1. Introduction

The Interstellar Medium (ISM) can be described as a clumpy, inhomogeneous three-phase medium (McKee & Ostriker, 1977: MO77). The cold neutral phase ($T \sim 80$ K, $n \sim 40$ cm^{-3}) is represented by the cores of molecular clouds which are enveloped by a warm neutral to slightly ionized medium ($T \sim 8000$ K, $n \sim 0.3$ cm^{-3}). These two components are in pressure equilibrium if the gas is externally heated and can cool radiatively (Field et al., 1969). According to MO77 they are embedded in a third hot, dilute phase of the ISM ($T \sim 10^6$ K, $n \sim 10^{-3}$ cm^{-3}). This component, which is produced by supernova (SN) explosions, can originally not be in pressure equilibrium with the colder phases and has therefore to expand vehemently. During this expansion, shocks arise, penetrate through and interact with the ambient clumpy ISM. In OB associations the sequential SNe accumulate and form a simple giant hot gas bubble, called superbubble, that expands preferentially towards the

halo and occupies a large volume (Norman & Ikeuchi, 1989). In order to allow for a more efficient cooling of the superbubble gas the evaporation of incorporated clouds are invoked (Silich et al., 1994). This evaporation of cloud material should be caused by heat conduction of electrons from the hot to the cold gas. Our aim is to investigate the interaction between the streaming hot plasma of the ISM and the molecular clouds in order to determine the rôle of heat conduction during the cloud evolution.

A situation described above comes into play in many astrophysical phenomena. As an example *High-Velocity Clouds* (HVCs) are radially falling towards the galactic disk (see Wakker & van Woerden, 1997, for a recent review) and penetrate through the hot halo gas (Kerp et al., 1996). Single HVCs are grouped together in complexes which can be found all over the sky. Interferometer measurements of the 21 cm Hi line at 1′ resolution reveal the substructure of single complexes that consist of several small clumps embedded in larger emission regions (Wakker & Schwarz, 1991). This, along with their line widths led Wakker & Schwarz conclude that the HVCs have a multi-phase structure consisting of a cold, dense core and a warmer, more tenuous envelope. Distance measurements for the cloud complexes remain difficult. For at least two of them upper limits for their distance are available (Danly et al. 1993; Keenan et al. 1995; van Woerden et al. 1997). These estimates reveal that they belong to the hot galactic halo. Although the origin of most of the complexes is still speculative (Blitz et al., 1999), HVCs are therefore a classic example for structures moving through a hot plasma.

Another example for the scenario described above are the much more massive and larger speculative proto-globular cluster clouds (PCCs) with temperatures near 10^4 K and densities several hundred times that of the surrounding gas. Therefore they are gravitationally unstable at masses larger than 10^6 $M_\odot$. These clouds originate from condensations of thermally unstable gas with temperatures of some million Kelvin in the early epoch of galaxy formation and can be envisaged as progenitors of globular clusters (Fall & Rees, 1985). The PCCs had to resist their gravitational collapse for a sufficient time until star formation ignites. On the other hand, they are accelerated in the gravitational potential of the forming protogalaxy and therefore move through a hot plasma where they become subject to the growth of Kelvin-Helmholtz (KH) and Rayleigh-Taylor (RT) instabilities (Drazin & Reid, 1981).

Stable models for both, HVCs and PCCs, assuming hydrostatic and thermal equillibrium consist of large temperature and density gradients at the surfaces of the clouds where the energy densities of the hot, tenuous ISM and the warm, dense cloud become equal. Because of this large temperature gradient and the high temperature of the ambient

medium of the order of some million Kelvin, heat conduction has to play an substantial rôle on the evolution of such clouds.

2. Heat conduction

Heat conduction results in an additional heat flux $\vec{q}$, that can be written in the classical case where the mean free path of the electrons is small compared to the temperature scaleheight as (Spitzer, 1962)

$$\vec{q}_{\mathrm{class}} = -\kappa \cdot \vec{\nabla} T \tag{1}$$

with

$$\kappa = \frac{1.84 \cdot 10^{-5} \, T^{5/2}}{\ln \Lambda} \ \mathrm{erg \ s^{-1} \ K^{-1} \ cm^{-1}} \tag{2}$$

where the Coulomb logarithm is

$$\ln \Lambda = 29.7 + \ln \left[\frac{T_e}{\sqrt{n_e} \, 10^6 \mathrm{K}} \right] \tag{3}$$

with the electron density n_e and the electron temperature T_e, respectively. The diffusion approximation for the heat flux breaks down if the mean free path becomes comparable or even greater than the temperature scaleheight. A common approach is to use a flux limited form, socalled "saturated" heat flux. This takes charge conservation into account and yields results in good agreement with more sophisticated treatments (e.g. Max et al., 1980) and with numerical simulations of laser heated plasmas (Morse & Nielsen 1973; Manheimer & Klein 1975). This saturated heat flux takes the form (Cowie & McKee, 1977: CM77)

$$|\vec{q}_{\mathrm{sat}}| = 5 \, \Phi_s \, \rho c^3 \tag{4}$$

where c is the sound velocity and Φ_s is a number less than or of the order of unity which embodies some uncertainties concerning the flux limited treatment ($\Phi_s = 1$ in our calculation). In order to get a smooth transition between both the classical and the saturated regime we used the analytical form by Slavin & Cox (1992)

$$\vec{q} = |\vec{q}_{\mathrm{sat}}| \left(1 - \exp \left[-\frac{\vec{q}_{\mathrm{class}}}{|\vec{q}_{\mathrm{sat}}|} \right] \right) \tag{5}$$

This guarantees that the smaller flux is taken if both differ significantly. As a criterion to separate both cases for a cloud of radius R embedded in a hot gas with temperature T_f, electron density n_{ef} and thus the

conductivity κ_f, CM77 introduced a global saturation parameter which is essentially the ratio of the electron mean free path to the cloud radius

$$\sigma_0 = \frac{0.08 \, \kappa_f \, T_f}{\Phi_s \, \rho_f \, c_f^3 \, R} = \frac{1.23 \cdot 10^4 \, T_f^2}{n_{ef} \, R} \; . \tag{6}$$

For $\sigma_0 < 0.027/\Phi_s$ material condenses onto the cloud because radiative losses exceed the conductive heat input. For $0.027/\Phi_s < \sigma_0 \leq 1$ the clouds suffer classical evaporation, while for $\sigma_0 > 1$ the evaporation is saturated. The classical evaporation rate is given by CM77:

$$\dot{m}_{\mathrm{class}} = \frac{16 \, \pi \, \mu \, \kappa_f \, R}{25 \, k_B} \; , \tag{7}$$

while for the saturated case, $\dot{m}_{\mathrm{class}}$ is multiplied by a function $w(\sigma_0)$ (Dalton & Balbus, 1993) which lowers the mass loss rate for $\sigma_0 > 0.01$.

3. Hydrodynamic Simulations

The evolution of clouds in the subsonic stream of a hot plasma is studied by two-dimensional hydrodynamical simulations. For this the Eulerian equations are solved on a rectangular cylindrical symmetric "staggered grid" which is second order in space. The boundary conditions are chosen in a manner that material can flow out of the computational domain through the upper and right boundary. The physical parameters of the lower boundary that is also the symmetry axis are mirrored. The parameters, density and temperature, at the left boundary keep their initial values. Also the flow of the plasma is initialized by setting the velocity of the left boundary to the requested value. In order to follow the condensation of the streaming material onto the cloud a new quantity "colour" was introduced. The value of this new quantity is set in each cell to the density of hot ISM. At the beginning of the calculation only the cells not belonging to the cloud have a colour unequal to zero with a value equal to its density. During the calculation this quantity is advected like the others as e.g. density or energy density. For the advection we used the monotonic transport of van Leer (1977). The Poisson equation for self-gravity was solved if the new evaluated gravitational potential differs from the old one by more than 10^{-4}. The energy equation is extended by heating, cooling and heat conduction, the latter one being the divergence of the heat flux (equ. 5). The adopted cooling function assumed collisional ionisation equilibrium and is a combination of the function introduced by Böhringer & Hensler (1989) for $T > 10^4$K and by Dalgarno & McCray (1972) for the lower

temperature regime. The heating function considers heating by cosmic rays, X-rays and the photoelectric effect on dust grains.

3.1. Theoretical Model

The initial profile of the cloud is generated for hydrostatic and thermal equilibrium. After setting the temperature T_{ISM} and particle density n_{ISM} of the hot and tenuous outer medium the energy density e_{ISM} of the plasma is known. The density and temperature profile of the cloud is calculated by integrating the equations of hydrostatic and thermal equilibrium from inside out using the core temperature of the cloud as the inner boundary condition and is truncated when the energy density reaches e_{ISM}. The model parameters are given in Table I. The parameters σ_0 and the evaporation timescale τ_{eva} are only defined for the simulation with heat conduction. The hot gas streams with 0.3 Mach. The resulting σ_0 for the simulation with heat conduction achieves a moderate saturation; the evaporation timescale τ_{eva} is calculated from equation (7) correspondingly. The dynamical timescale as defined to be the sound travel time over one cloud radius, is 16.2 Myr. For the grid 440×160 cells are used in the simulation with heat conduction and 640×200 cells for the simulation without heat conduction. Thus, the spatial resolution amounts to 1.25 pc/cell.

Table I. Model parameters of the simulation

T_{ISM} (K)	n_{ISM} (cm^{-3})	v_{ISM} (km s^{-1})	R_{cld} (pc)	M_{cld} M$_\odot$	density contrast	σ_0	$\tau_{\mathrm{eva}} = M/\dot{m}$ Myr
$5.6 \cdot 10^6$	$6.6 \cdot 10^{-4}$	107.4	41.3	$6.4 \cdot 10^4$	$1.2 \cdot 10^4$	10.5	279

4. Results

The inclusion of heat conduction has the tendency to stabilize massive and large clouds. This is illustrated comparing the density contours at the same times (30 Myr and 50 Myr after the beginning of the calculations) for the simulations without (Fig. 1) and with heat conduction (Fig. 2). Without heat conduction the edge of the cloud is torn by KH instability already shortly after the beginning when the density contrast is lowered. Also a very complex velocity structure with many vortices behind the cloud has formed. On the other hand, heat conduction suppresses large scale KH instabilities and only a single large circulation in

the slipstream of the cloud is visible. This behaviour can be understood
if the conducting electrons move along the temperature gradient, i.e.
radially toward the cloud. This leads to a deceleration of the contact
interphase so that the relative velocity decreases below a critical value
that determines the onset of KH instabilities. Also the inner parts of the
clouds develop differently. While in both simulations the cores remain
very dense, the model without heat conduction develops a compound
envelope, with a radially decreasing density and a diluted outer part of
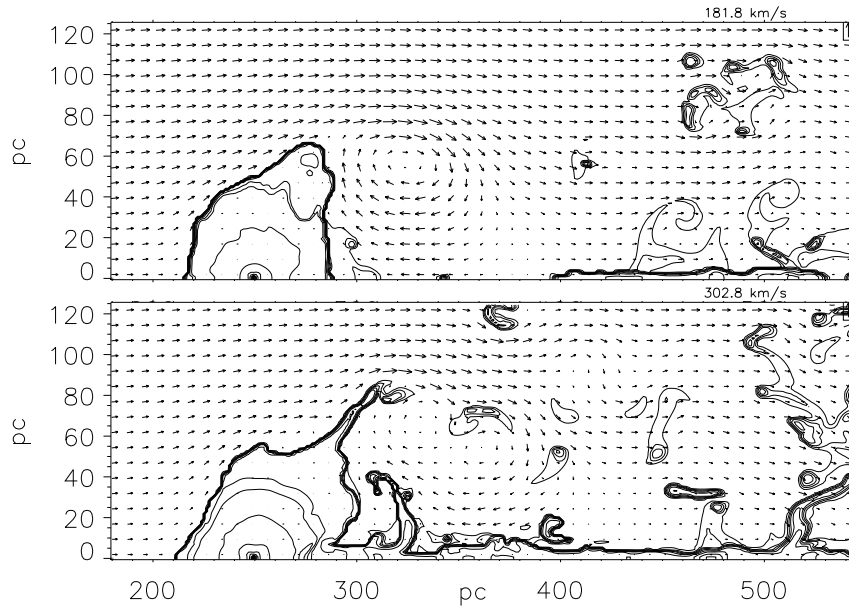material that is only slightly gravitationally bound.

Figure 1. Density contours for the simulation without heat conduction at 30 Myr
(upper panel) and 50 Myr (lower) after the beginning of the calculation. The con-
tour lines represent 5, 10, 50, 100,... $\times \rho_{\mathrm{ISM}}$. The velocity arrows scale linearly with
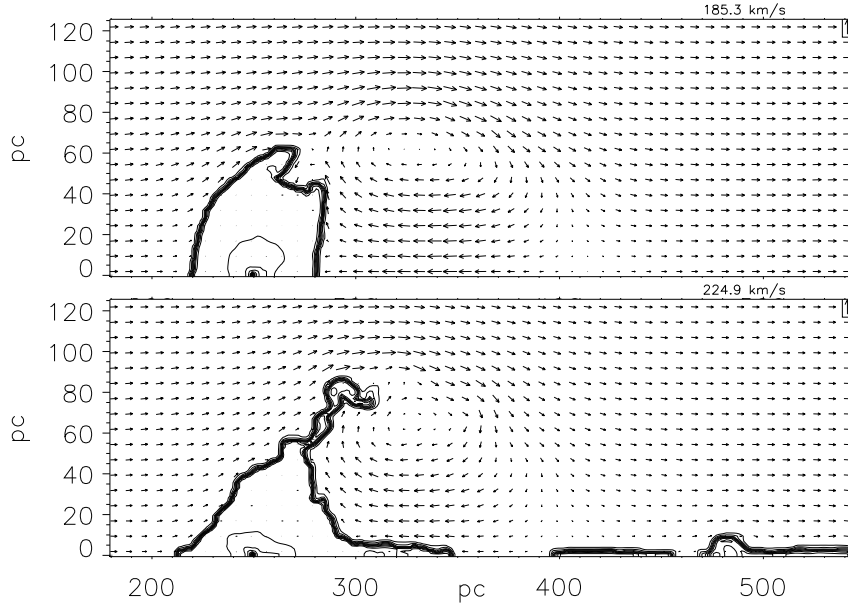respect to the maximum velocity shown in the upper right.

Figure 2. Density distribution for the simulation with heat conduction at 30 Myr (upper panel) and 50 Myr (lower) after the beginning of the calculation. The contour levels are the same as in Fig. 1

The cloud model with heat conduction remains more compact with bound edges. In regions where the heat conduction exceeds the cooling the density distribution is homogenized while in very dense regions like e.g. near the core the density structure is unaffected by heat conduction. The tendency to smooth out temperature and density inhomogenities is also the reason why KH instability is suppressed. At the edge of the cloud an interface builds up which broadens the transition region from the cloud to the outer medium. This transition region is visible in Fig. 2 as a broad band of contour lines where the former steep temperature and density gradients are diminished. Within this interface at the cloud's surface the sheer velocity is therefore lowered and the KH instability is reduced, by this, enabling material from the flow to settle onto the cloud. This difference is clearly discernible in Fig. 3. After 76 Myr almost 160 $M_\odot$ have stuck into the cloud what amounts to almost 0.3% of the total cloud mass. The simulation without heat conduction shows an accretion that is only 1/3 of that one with heat conduction because the accreted material is stripped off from the cloud again before it can be mixed with deeper layers of the cloud. The evolution of the total mass (see Fig. 4) differs only marginally. Long-term simulations have to be performed in order to investigate whether the total mass reaches a constant value. Nevertheless, it is obvious, that the cloud evolution is not suffering evaporation at that stage as claimed by CM77.

The mass-loss rate corresponding to the analytical expression given by equ. 7 is by far too high. The question has to be addressed whether the assumptions by CM77 are valid in such a more realistic case in which instabilities occur and a streaming hot plasma serves as an infinite reservoir. In order to answer it, a parameter study covering both the condensation and evaporation regime proposed by CM77 has to be performed and investigations must include a higher spatial resolution.
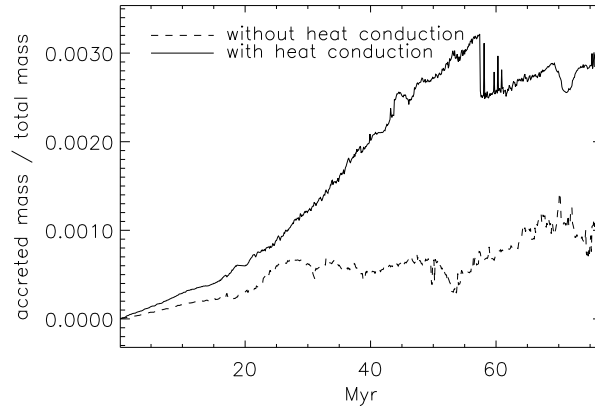

Figure 3. Evolution of the accretion of the streaming material onto the cloud.
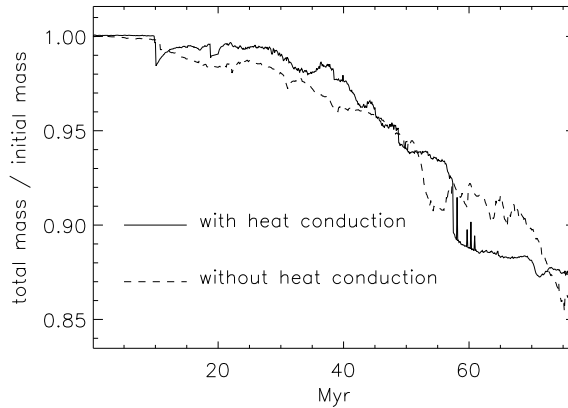

Figure 4. Evolution of the gravitationally bounded mass with the regard to the initial mass.

References

Blitz L., et al.: 1999, *ApJ* **514**, 818

Böhringer H., Hensler G.: 1989, *A&A* **215**, 147

Cowie L.L., McKee C.F.: 1977, *ApJ* **211**, 135

Dalgarno A., McCray R.A.: 1972, *Ann. Rev. Ast. Ap.* **10**, 375

Dalton W.W., Balbus S.A.: 1993, *ApJ* **404**, 625

Danly L., Albert C.E., Kuntz K.D.: 1993, *ApJ* **416**, L29

Drazin P.G., Reid W.: 1981, *Hydrodynamic Stability*, Cambridge Univ. Press, Cambridge, S.16

Fall S.M., Rees M.J.: 1985, *ApJ* **298**, 18

Field G.B., Goldsmith D.W., Habing H.J.: 1969, *ApJ* **155**, L149

Keenan F.P., et al.: 1995, *MNRAS* **272**, 599

Kerp J., et al.: 1996, *A&A* **312**, 67

Manheimer W.M., Klein H.H.: 1975, *Phys. Fluids* **18**, 1299

Max C.E., McKee C.F., Mead W.C.: 1980, *Phys. Fluids* **23**, 1620

McKee C.F., Ostriker J.P.: 1977, *ApJ* **218**, 148

Morse R.L., Nielsen C.W.: 1973, *Phys. Fluids* **16**, 909

Norman C.A., Ikeuchi S.: 1989, *ApJ* **345**, 372

Silich S.A., Franco J., Palouš J., Tenorio-Tagle G.: 1994, in Proc. of the first IAC-RGO meeting *Violent Star Formation*, ed. Tenorio-Tagle G., Cambridge Univ. Press, Cambridge, S.162

Slavin J.D., Cox D.P.: 1992, *ApJ* **392**, 131

Spitzer L.: 1962, *Physics of Fully Ionized Gases*, Interscience, New York

van Leer B.: 1977, *J. Comp. Phys.* **23**, 276

van Woerden H., et al.: 1997, in Proc. of the IAU Coll. No.166 *The Local Bubble and Beyond*, eds. D. Breitschwerdt, M.J. Freyberg, J. Trümper, Springer, New York, S.467

Wakker B.P., Schwarz U.J.: 1991, *A&A* **250**, 484,

Wakker B.P., van Woerden H.: 1997, *Ann. Rev. Ast. Ap.* **35**, 217

Address for Offprints:
vieser@astrophysik.uni-kiel.de